

## Structural and AC Impedance Studies on Nanocomposite Polymer Electrolytes Based on Poly( $\epsilon$ -caprolactone)

K. Sownthari, S. Austin Suthanthiraraj

Department of Energy, University of Madras, Guindy Campus, Chennai 600025, India

Correspondence to: K. Sownthari (E-mail: sownthari@gmail.com)

**ABSTRACT:** Nanocomposite polymer electrolyte (NCPE) films of [75 wt % poly( $\epsilon$ -caprolactone) : 25 wt % zinc triflate] +  $x$  wt % nanofiller  $\text{Al}_2\text{O}_3$  ( $x = 1, 3, 5, 7$ ) were prepared by solution cast technique. Such NCPE films were characterized using Fourier transform infrared and AC impedance spectroscopic techniques. Complexation of polymer with salt and nanofiller was revealed from FTIR analysis. On the other hand, an apparent increase in the number density of charge carriers upto 5 wt % loading of the nanofiller was also confirmed. Furthermore, AC impedance spectroscopic studies have shown that ionic conductivity increases with the addition of  $\text{Al}_2\text{O}_3$  and reaches a maximum of  $2.5 \times 10^{-5} \text{ S cm}^{-1}$  at room temperature for 5 wt % loading of nanofiller. The dielectric behavior of all the synthesized samples has also been analyzed and presented. © 2014 Wiley Periodicals, Inc. *J. Appl. Polym. Sci.* **2014**, *131*, 40524.

**KEYWORDS:** batteries and fuel cells; dielectric properties; spectroscopy

Received 26 October 2013; accepted 28 January 2014

DOI: 10.1002/app.40524

### INTRODUCTION

Polymer electrolytes are generally formed by the dissolution of a dopant salt within a polymer matrix containing polar groups such as O, N, S, F, and so on, whereas the most common polymer host employed in the field of polymer electrolytes is poly(ethylene oxide) (PEO), after the first successful work reported by Wright in 1970s.<sup>1</sup> Since a polymer electrolyte has several advantages like geometrical flexibility, ease of thin film formation, mechanical stability, and many others, over traditional liquid electrolytes, research on polymer electrolytes has attracted a large number of researchers in recent years.

Several polymers such as PEO, poly(vinylidene fluoride) (PVdF), poly(methyl methacrylate) (PMMA), poly(vinyl chloride) (PVC), poly(acrylonitrile) (PAN), and similar systems<sup>2</sup> were utilized in the preparation of polymer electrolytes as a host polymer. Over the evolution of technology, efforts are being taken to employ biodegradable polymers like chitosan, gelatin, poly(vinyl alcohol) (PVA), poly( $\epsilon$ -caprolactone) (PCL) as a host for the synthesis of new polymer electrolytes.<sup>3</sup> In the present study, PCL has been considered as the host for the development of a new polymer electrolyte system. The chosen polymer PCL is biodegradable and characterized with a low glass transition temperature and hence it may yield promising and useful polymer electrolytes as well. Among the various available dopant salts such as triflate salts of lithium, zinc, sodium, magnesium and  $\text{LiClO}_4$ ,  $\text{NH}_4\text{SCN}$ ,  $\text{LiBF}_4$ ,  $\text{H}_3\text{PO}_4$ , and many more, zinc triflate was chosen to be the dopant salt, since

zinc is less toxic, stable, and has a high specific energy as reported by Kumar and Sampath.<sup>4</sup>

The only disadvantage of polymer electrolyte in its pure form is its low conductivity. Nanocomposite polymer electrolytes (NCPEs) are a class of polymer electrolytes in which incorporation of nanofiller into the polymer-salt complex not only increases its electrical conductivity but also improves the overall thermal, mechanical, and electrochemical stability. A variety of inorganic nanofillers have been investigated so far which include  $\text{Al}_2\text{O}_3$ ,  $\text{SnO}_2$ ,  $\text{SiO}_2$ ,  $\text{TiO}_2$ ,  $\text{CeO}_2$ ,  $\text{BaTiO}_3$ , etc.,<sup>5</sup> whereas the first and most extensive efforts have been reported in the case of  $\text{Al}_2\text{O}_3$  filler till date.

Although, the search for better conducting materials has been the primary interest of researchers nowadays, it is also important to understand their molecular interactions, conduction mechanism, and relaxation processes occurring especially within the NCPE system of interest. In this context, Fourier transform infrared (FTIR) spectroscopy helps in understanding the molecular level interactions which is necessary in order to ascertain the complexation of polymer, salt, and nanofiller. Conductivity and relaxation processes associated with conductivity could be evaluated effectively using AC impedance spectroscopy which may provide valuable information about the dielectric response of the material.

Therefore, in the present study, a series of NCPEs comprising PCL and zinc triflate with varying concentrations of  $\text{Al}_2\text{O}_3$  nanofiller have been prepared and characterized using FTIR and AC impedance spectroscopic analyses. The effect of

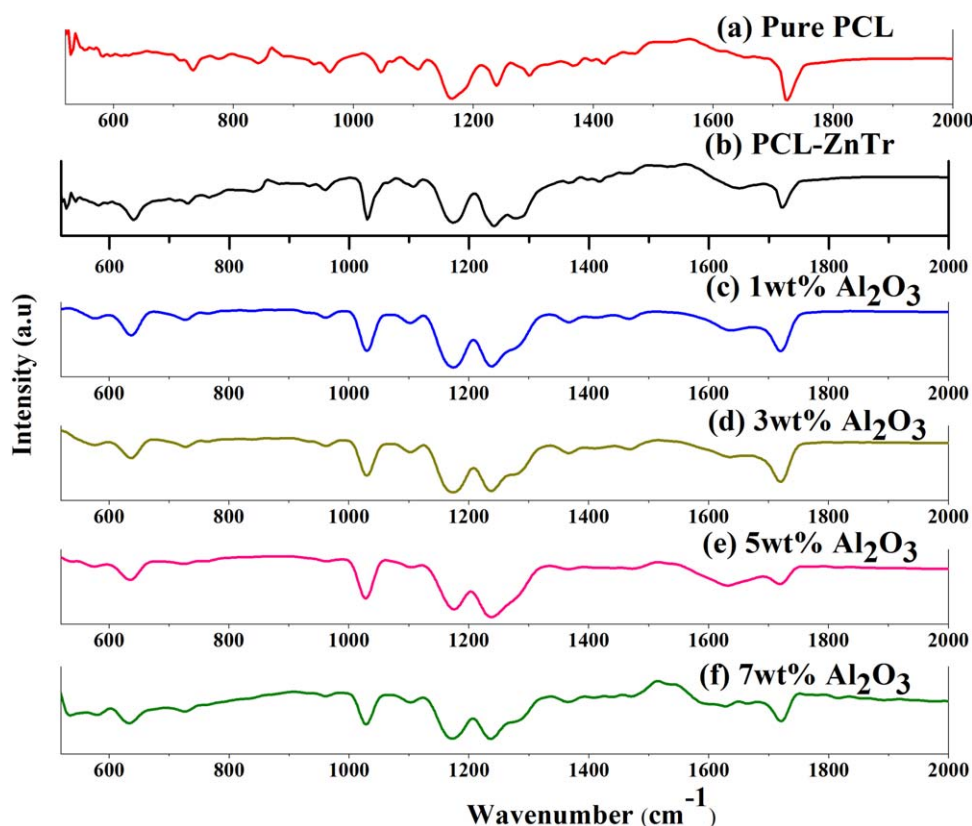


**Figure 1.** FTIR spectra for (a) pure PCL, (b) PCL–ZnTr complex (75 : 25 wt %), (c–f) NCPE with 1, 3, 5, 7 wt %  $\text{Al}_2\text{O}_3$ . [Color figure can be viewed in the online issue, which is available at [wileyonlinelibrary.com](http://wileyonlinelibrary.com).]

incorporation of  $\text{Al}_2\text{O}_3$  nanofiller and its concentration on structure, conductivity, and dielectric relaxation processes of the prepared NCPEs has also been investigated.

## EXPERIMENTAL

### Materials and Method

PCL with  $M_n = 80$  kDa, ZnTr with  $M_w = 363.53$   $\text{g mol}^{-1}$  and  $\text{Al}_2\text{O}_3$  nanopowder of particle size  $<50$  nm were procured from Sigma-Aldrich, USA. ZnTr and  $\text{Al}_2\text{O}_3$  nanopowder were dried at  $100^\circ\text{C}$  for an hour prior to use, while PCL was used as received. Appropriate quantities of  $\text{Al}_2\text{O}_3$  nanopowder in 1, 3, 5, and 7 wt % were incorporated into the optimized polymer-salt composition i.e., 75 : 25 wt % of PCL : ZnTr complex. Mixtures containing PCL, ZnTr, and  $\text{Al}_2\text{O}_3$  nanopowder in the common solvent tetrahydrofuran (THF) were stirred continuously for several hours at room temperature in order to obtain a homogenous viscous solution which was then solvent cast onto a glass petri dish and maintained at  $50^\circ\text{C}$  in order to allow THF to evaporate and then vacuum dried at  $50^\circ\text{C}$  for 15 h. These films were further dried slowly at room temperature inside a desiccator for 2 days so as to remove any traces of the solvent. Self-standing translucent films thus obtained were stored in a dry desiccator for further measurements.

### Characterization Techniques

FTIR spectra were recorded for each neat film specimen in the transmission mode at room temperature using a Perkin–Elmer RX1 spectrophotometer with a wavenumber resolution of 4

$\text{cm}^{-1}$  over the wavenumber range  $400\text{--}4000$   $\text{cm}^{-1}$ . However, for the sake of better clarity only those spectral components of the region of  $500\text{--}2000$   $\text{cm}^{-1}$  were presented in this manuscript.

AC impedance measurements were carried out in the frequency range 1 MHz–20 Hz with an excitation signal of 500 mV using a computer-controlled Hewlett-Packard Model HP 4284A Precision LCR Meter at room temperature ( $25^\circ\text{C}$ ). The appropriate specimens of NCPEs were sandwiched between a pair of polished stainless steel (SS) disks maintained under dry nitrogen atmosphere so as to prevent undesirable atmospheric water vapor during impedance measurements. The electrical conductivity was calculated using the equation:

$$\sigma = \frac{t}{R_b A} \quad (1)$$

Here,  $t$  is the thickness of the sample,  $R_b$  the bulk resistance, and  $A$  is the area of contact. The value of  $R_b$  was obtained from the observed low frequency intercept of the semicircle on the real axis of the impedance plot.

## RESULT AND DISCUSSION

### Fourier Transform Infrared Spectroscopic Studies

Figure 1 shows the series of FTIR spectra in the case of pure PCL, PCL–ZnTr complex, and NCPE specimens with different loading of  $\text{Al}_2\text{O}_3$  nanofiller recorded in the wave number range  $500\text{--}2000$   $\text{cm}^{-1}$ . Pure PCL has a predominant peak at  $1720$   $\text{cm}^{-1}$  which corresponds to the stretching of carbonyl group.

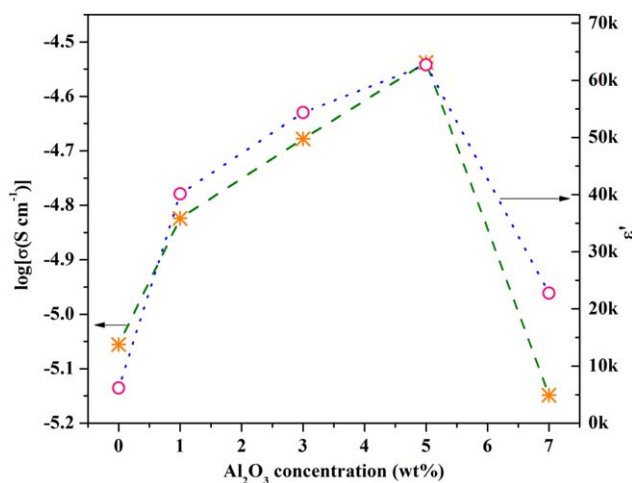


**Figure 2.** Variation of electrical conductivity and dielectric constant at a fixed frequency of 100 Hz of NCPEs as a function of  $\text{Al}_2\text{O}_3$  concentration. [Color figure can be viewed in the online issue, which is available at [wileyonlinelibrary.com](http://wileyonlinelibrary.com).]

Other peaks at 1172, 1238, 1292, 1165, 1190, and 960  $\text{cm}^{-1}$  were attributed to the symmetric and asymmetric COC stretching, C—O and C—C stretch in crystalline and amorphous phases, OC—O stretching, and  $\text{CH}_2$  rocking, respectively.<sup>6</sup>

Some specific changes were noticed with the addition of salt into the polymer PCL in the case of the optimized composition as shown in Figure 1(b). Since the carbonyl group is the strong  $e^-$  donor within this polyester, a shoulder peak appears at 1650  $\text{cm}^{-1}$  which corresponds to the coordination of the  $\text{Zn}^{2+}$  ion with the oxygen of the carbonyl group.<sup>7</sup> Peak observed at 1033  $\text{cm}^{-1}$  was attributed to the symmetric ( $\text{SO}_3$ ) stretching mode of free triflate ion. The bands noticed at 634 and 577  $\text{cm}^{-1}$  correspond to the symmetric ( $\text{SO}_3$ ) deformation and asymmetric ( $\text{CF}_3$ ) deformation of free triflate.<sup>8</sup> The peak area of free triflate directly denotes the charge density of triflate ions.

With the incorporation of  $\text{Al}_2\text{O}_3$  nanofiller, no additional peaks were observed in the spectra of NCPEs as evident from Figure 1(c–f). An apparent change in the intensity of peaks at 1033 and 634  $\text{cm}^{-1}$  has been noticed. The peak intensity increases upto 5 wt % loading of the nanofiller, which may also correspond to the increase in the number density of charge carriers. The peak position of the shoulder peak at 1650  $\text{cm}^{-1}$  also changes confirming the Lewis acid–base type interaction of the nanofiller with the polymer–salt complex in the manner explained by Dissanayake et al.<sup>9</sup> Therefore, it is inferred that NCPE with 5 wt %  $\text{Al}_2\text{O}_3$  has the largest number of free triflate ions which also means a large number of free  $\text{Zn}^{2+}$  ions.

### AC Impedance Studies

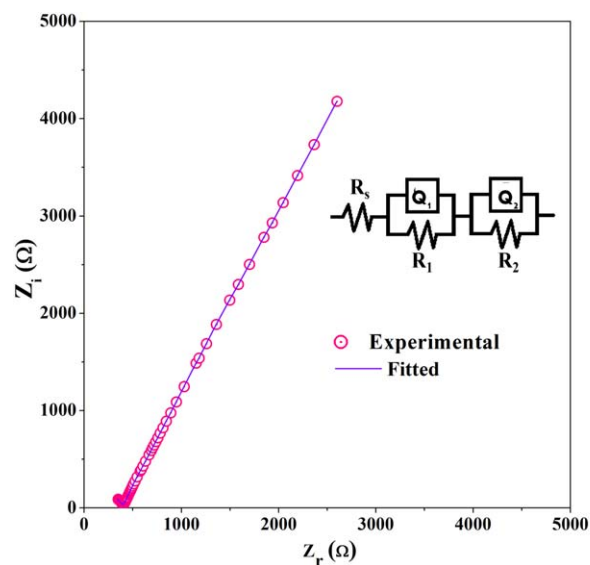
AC impedance measurements were carried out on all the prepared samples with a view to understand the behavior of electrical conductivity and conduction mechanism of all the synthesized NCPEs. The value of conductivity increases from  $8.8 \times 10^{-6} \text{ S cm}^{-1}$  observed for 0 wt %  $\text{Al}_2\text{O}_3$  to a maximum of  $2.5 \times 10^{-5} \text{ S cm}^{-1}$  at room temperature for 5 wt % loading of nanofiller as shown in Figure 2 along with the variation of

dielectric constant. This aspect may be attributed to an increase in the number of charge carriers as observed from FTIR analysis. Further increase in the content of the filler leads to a decrease in the observed conductivity. At a lower concentration of  $\text{Al}_2\text{O}_3$  nanofiller, the filler may act like a plasticizer, thereby reducing the crystallinity of the polymer electrolyte and providing conduction pathways for the mobile ions. Furthermore, the number of charge carriers also increases as the presence of the filler enhances the process of salt dissociation. At higher concentrations of the filler (i.e., at 7 wt % of nanofiller), the mobility of charge carriers may be affected by the presence of an excess filler which could stiffen the polymer chain thereby hindering the conduction pathways of mobile ions.<sup>10</sup> This concept was well supported by the fact that the observed electrical conductivity depends both on the number density and mobility of charge carriers, as

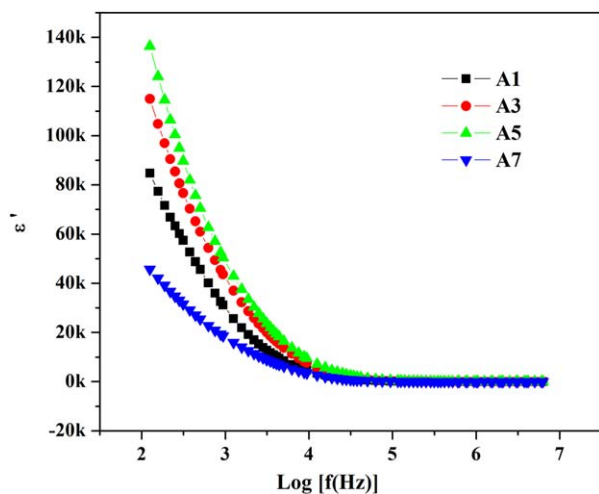
$$\sigma = nq\mu \quad (2)$$

Figure 3 shows the experimental and fitted impedance spectra in the case of a representative film namely the best conducting sample with 5 wt % loading of  $\text{Al}_2\text{O}_3$  nanofiller and its possible equivalent circuit. Here,  $R_s$  represents the electrolyte resistance which is in series with the parallel combination of charge transfer resistance ( $R_1$ ) and constant phase element (CPE) which is an imperfect capacitor represented as  $Q_1$ , in this case. The CPE used in the place of a capacitor represents the electrode roughness, porosity, and inhomogeneity of the NCPE system.<sup>11</sup> CPE has an  $n$  value ranging from 0 to 1. The case where  $n = 1$  describes an ideal capacitor whereas the case where  $n = 0$  describes a pure resistor. In the present case, the value of  $n$  is found to be 0.8. Therefore, the formation of CPE implies the non-Debye behavior of the present NCPE system. Moreover, the parallel combination of  $Q_2$  and  $R_2$  denotes the presence of electrode/electrolyte interfacial phenomenon.

Figure 4 shows the variation of dielectric constant,  $\epsilon'$ , as a function of frequency. Dielectric constant denotes the measure of



**Figure 3.** The impedance spectra of the best conducting sample with 5 wt %  $\text{Al}_2\text{O}_3$  nanofiller and its equivalent circuit. [Color figure can be viewed in the online issue, which is available at [wileyonlinelibrary.com](http://wileyonlinelibrary.com).]



**Figure 4.** Variation of dielectric constant,  $\epsilon'$  as a function of frequency. [Color figure can be viewed in the online issue, which is available at [wileyonlinelibrary.com](http://wileyonlinelibrary.com).]

charge stored or the amount of dipoles aligned in the direction of the electric field. In zero applied field, the electrolyte may have no net charge but an applied field exerts a force to push the positive charges in the direction of the field and negative charges in the opposite direction. The dipoles of the immobile polymer chains would also participate in this process via conformational changes contributing polarization. As seen from Figure 4, the dielectric response of the NCPE exhibits dispersion at the low frequency side and a tail at high frequency side. At low frequency, charges would have more time to migrate and accumulate at the electrode/electrolyte interface and thereby contribute to the observed dielectric constant. At high frequency, the periodic reversal of the applied field occurs very rapidly so that almost no charges were able to migrate in the direction of the field.<sup>12</sup>

The variation of dielectric constant at a fixed frequency of 100 Hz as a function of filler concentration is given in Figure 2 and

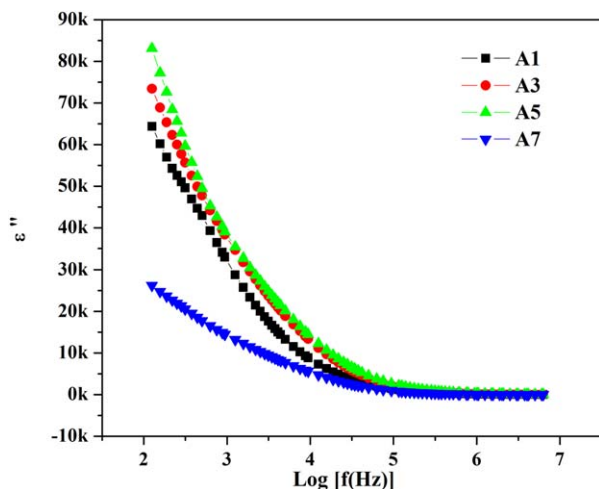


**Figure 5.** Variation of dielectric loss,  $\epsilon''$  as a function of frequency. [Color figure can be viewed in the online issue, which is available at [wileyonlinelibrary.com](http://wileyonlinelibrary.com).]

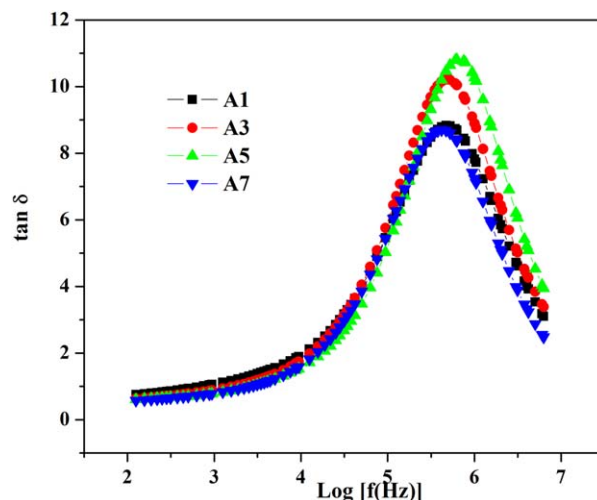


**Figure 6.** Variation of loss tangent as a function of frequency for different filler concentrations of NCPEs. [Color figure can be viewed in the online issue, which is available at [wileyonlinelibrary.com](http://wileyonlinelibrary.com).]

found to follow the same trend as that of electrical conductivity. This feature confirms the fact that the best conducting sample with 5 wt %  $\text{Al}_2\text{O}_3$  nanofiller has the highest number of charge carriers, as concluded from FTIR analysis.

The variation of dielectric loss as a function of frequency is given in Figure 5.

The applied alternating field makes the charges and polar group within the NCPE to swash back and forth in the direction of the field. If their oscillations were exactly in phase with the field, then no energy would be lost. However, permanent dipoles existing within the material have to rotate, realign in the direction of the applied field which would never be exactly in phase, and may interfere with each other, dissipating energy in the form of heat, contributing to dielectric loss. Greater the number of charge carriers, larger the amount of energy dissipated,<sup>13</sup> and could be observed well from Figure 5 as the best conducting sample with 5 wt % loading of filler has exhibited the maximum dielectric loss.

The dielectric relaxation process may be explained by loss tangent and expressed as

$$\tan \delta = \frac{\epsilon''}{\epsilon'} \quad (3)$$

Figure 6 shows the variation of loss tangent as a function of frequency for different filler concentrations of NCPE at room temperature. The relaxation peak becomes more intense and shifts toward higher frequency side with an increase in the filler concentration upto 5 wt %. Generally, the chain length of polymer PCL is so long that the bond rotation is favorable only at low frequency i.e., higher is the relaxation time.<sup>14</sup> But the presence of filler increases the disorder within the polymer network and thus the rotation becomes feasible, making a shift toward higher frequency side which means a shorter relaxation time. On increasing the filler concentration beyond 5 wt %, the presence of excess filler particles makes the polymer chain very rigid to allow any conformational changes and hence the relaxation



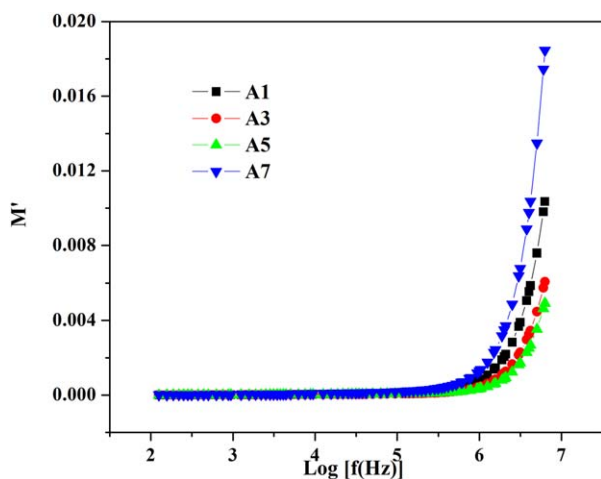


**Figure 7.** Variation of  $M'$  as a function of frequency. [Color figure can be viewed in the online issue, which is available at [wileyonlinelibrary.com](http://wileyonlinelibrary.com).]

occurs at a low frequency in conjunction with a higher relaxation time.

Electric modulus may be defined as the reciprocal of the complex relative permittivity as given below

$$M^* = \frac{1}{\epsilon^*} = M' + iM'' \quad (4)$$

where  $M'$  and  $M''$  are the real and imaginary parts of the electric modulus. Figures 7 and 8 show the variation of  $M'$  and  $M''$  as a function of frequency respectively.  $M'$  exhibits a long tail in the vicinity of zero at low frequency and sigmoidal step at high frequency. At low frequency the value of  $M'$  approaches zero and is attributed to the electrode polarization. When the filler concentration increases, the spectrum shifts toward higher frequency upto 5 wt % beyond which it reverses.

$M''$  exhibits the same trend as that of  $M'$ . Since the maximum of modulus spectra  $M''$  shifts toward higher frequency, with the increase of filler concentration, the mobile ions may have shorter relaxation time, as

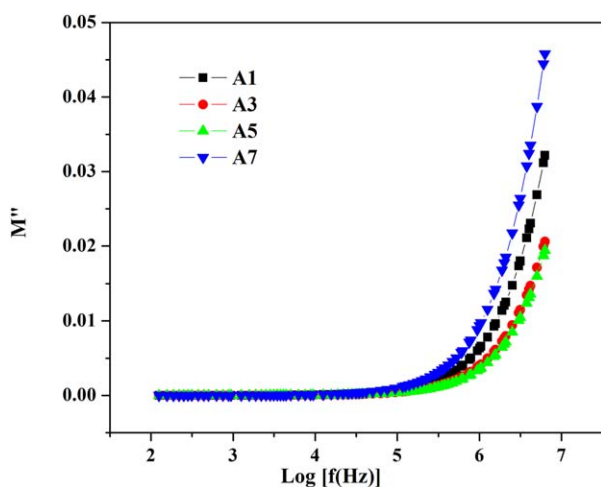


**Figure 8.** Variation of  $M''$  as a function of frequency. [Color figure can be viewed in the online issue, which is available at [wileyonlinelibrary.com](http://wileyonlinelibrary.com).]

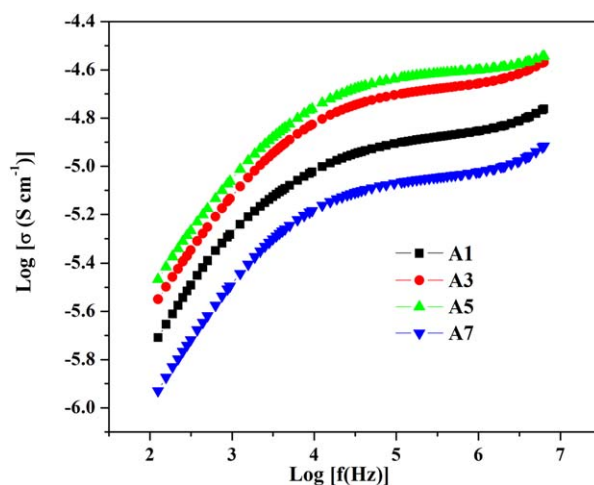


**Figure 9.** Frequency dependence of conductivity of NCPEs at room temperature. [Color figure can be viewed in the online issue, which is available at [wileyonlinelibrary.com](http://wileyonlinelibrary.com).]

$$\omega t = 1 \quad (5)$$

Moreover, the broad nature of these peaks may be associated with the non-Debye nature of the material with a distribution of relaxation times i.e., mobile ions may have more than one relaxation time.

The conductance spectra of all the NCPE samples are given in Figure 9 and show three distinct regions: a low frequency dispersive region, a mid frequency plateau, and high frequency dispersion. At a low frequency, ions have more time to accumulate at the electrode–electrolyte interface reducing the number of ions available for conduction and make a drop in the conductivity. At mid-frequency, the charges are frequency-independent and correspond to the conductivity of the bulk of the electrolyte. The extrapolation of this plateau to the  $y$ -axis represents dc conductivity ( $\sigma_{dc}$ ). It is noted that the value of  $\sigma_{dc}$  increases with nanofiller content upto 5 wt % loading of the filler above which the observed conductivity decreases. At the high

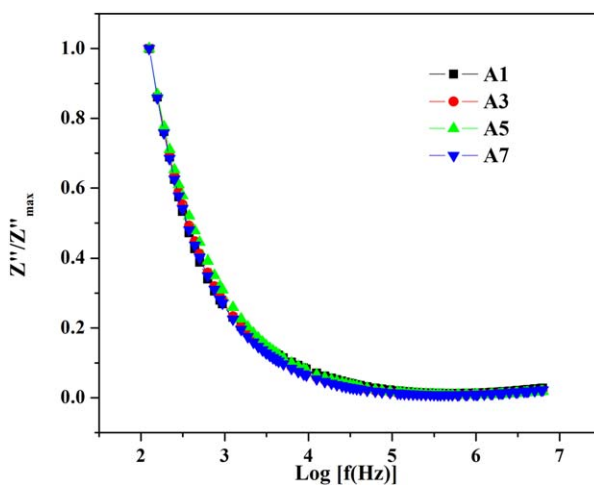


**Figure 10.** Normalized impedance spectra of NCPEs as a function of frequency. [Color figure can be viewed in the online issue, which is available at [wileyonlinelibrary.com](http://wileyonlinelibrary.com).]

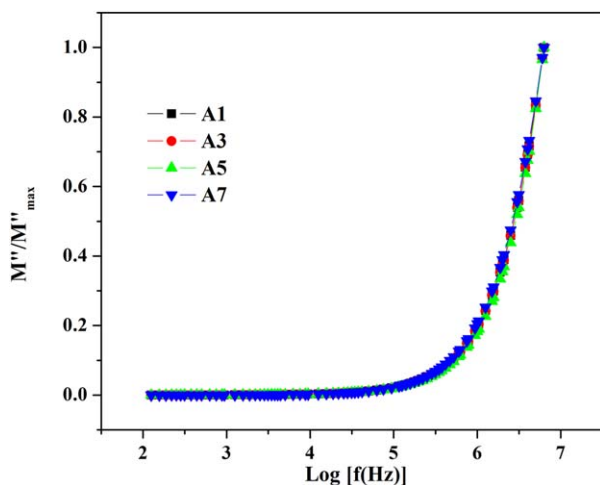


**Figure 11.** Normalized modulus spectra of NCPEs as a function of frequency. [Color figure can be viewed in the online issue, which is available at [wileyonlinelibrary.com](http://wileyonlinelibrary.com).]

frequency end, the mobility of ions is large enough and thus the conductivity increases with frequency.

Plots of normalized impedance and electric modulus as a function of frequency are given in Figures 10 and 11, respectively. It may be clearly seen that both these formalisms depict dispersion with no relaxation peak and the absence of relaxation peak may be attributed to the long range conductivity.<sup>15</sup> All the data points of both the formalisms tend to superimpose with each other for all the compositions considered and this feature indicates that the relevant dynamical processes of ions within the NCPE are same throughout the range of compositions studied.<sup>16</sup> The maxima of these formalisms occur at different frequencies thus confirming the non-Debye nature of these NCPEs.<sup>17</sup>

## CONCLUSIONS

A series of NCPEs were prepared by the incorporation of  $\text{Al}_2\text{O}_3$  nanofillers into the optimized PCL–ZnTr composition of 75 : 25 wt %. Complexation of polymer, salt, and filler was confirmed from FTIR studies. With an increase in the filler concentration, conductivity increases and reaches a maximum of  $2.5 \times 10^{-5} \text{ S cm}^{-1}$  for 5 wt % loading of filler. This aspect is mainly due to an apparent increase in the number density of charge carriers which was confirmed from FTIR and dielectric studies.

The increasing trend of dielectric constant matched well with the conductivity variation as a function of filler concentration. The various relaxation processes associated with conductivity mechanism were also analyzed during the investigation.

## ACKNOWLEDGMENTS

The financial support received in the form of INSPIRE-SRF programme from the Department of Science and Technology (DST), Government of India, New Delhi is gratefully acknowledged.

## REFERENCES

1. Wright, P. V. *Br. Polym. J.* **1975**, *7*, 319.
2. Agrawal, R. C.; Pandey, G.P. *J. Phys. D: Appl. Phys.* **2008**, *41*, 1.
3. Sownthari, K.; Suthanthiraraj, S. A. *Express Polym. Lett.* **2013**, *7*, 495.
4. Kumar, G. G.; Sampath, S. *Solid State Ionics* **2005**, *176*, 773.
5. Jung, S.; Kim, D. W.; Lee, S. D.; Cheong, M.; Nguyen, D. Q.; Cho, B. W.; Kim, H. S. *Bull. Korean Chem. Soc.* **2009**, *30*, 2355.
6. Woo, H. J.; Majid, S. R.; Arof, A. K. *Solid State Ionics* **2011**, *199*, 14.
7. Lin, C.-K.; Wu, I.-D. *Polymer* **2011**, *52*, 4106.
8. Kumar, D.; Hashmi, S. A. *Solid State Ionics* **2010**, *181*, 416.
9. Dissanayake, M. A. K. L.; Jayathilaka, P. A. R. D.; Bokalawala, R. S. P.; Albinsson, I.; Mellander, B.-E. *J. Power Sources* **2003**, 119–121, 409.
10. Zhou, J.; Fedkiw, P. S. *Solid State Ionics* **2004**, *166*, 275.
11. Guler, F. G.; Sarac, A. S. *Express Polym. Lett.* **2011**, *5*, 493.
12. Polu, A. R.; Kumar, R. *Bull. Mater. Sci.* **2011**, *34*, 1063.
13. Woo, H. J.; Majid, S. R.; Arof, A. K. *Mater. Chem. Phys.* **2012**, *134*, 755.
14. Khair, A. S. A.; Arof, A. K. *World Acad. Sci. Eng. Technol.* **2011**, *59*, 23.
15. Mitra, S.; Sampath, S. *Macromolecules* **2005**, *38*, 134.
16. Aziz, S. B.; Abidin, Z. H. Z.; Arof, A. K. *Express Polym. Lett.* **2010**, *4*, 300.
17. Ramya, C. S.; Savitha, T.; Selvasakarapandian, S.; Hirankumar, G. *Ionics* **2005**, *11*, 436.